Strains in epitaxial films: The general case

P. M. Marcus
IBM Research Center, Yorktown Heights, New York 10598

F. Jona
Department of Materials Science and Engineering, State University of New York, Stony Brook, New York 11794-2275
(Received 26 September 1994)

A procedure is given for the calculation of the complete strain tensor of a film in pseudomorphic or coherent epitaxy on an arbitrary substrate. In the general case the misfit between the film and substrate determines three in-plane strain components. The elastic equations of the film then determine the three out-of-plane components. Quantitative low-energy electron diffraction can find the structure of bulk layers of a metal film; hence strain analysis can use the measured structure to obtain information about the elastic constants of the material of the film. The procedure is applied to two examples of observed general pseudomorphic epitaxy and to one example of possible general pseudomorphic epitaxy from a list of closely matched bcc and fcc surfaces. The concept of an epitaxial line, which plots the geometry of a film under strain as the substrate is changed in scale, is generalized to an arbitrary pair of film-substrate surfaces.

I. INTRODUCTION

Pseudomorphic or coherent epitaxy of ultrathin crystalline films on crystalline substrates forces a unit mesh[1] of the film to take the dimensions of a substrate surface unit mesh. This clamping of the film by the substrate produces well-defined strain in the film plane homogeneous throughout the bulk part of the film, which is sometimes substantial and can be tensile as well as compressive. These strains can play an important role in the properties of the film material, e.g., they can stabilize phases which are not available macroscopically, and can also provide interesting information about the film material, e.g., about ratios of elastic constants. In order to obtain this information one needs to measure strain components in the bulk of the film. Ultrathin films are just a few atomic layers thick, but for metal films the bulk strain frequently starts at the third layer below the surface and is measurable by quantitative low-energy electron diffraction (QLEED). Hence strained bulk behavior can be measured in many epitaxial systems by growing pseudomorphic epitaxial films of six layers or more. The measurement of strain in epitaxial films depends both on the ability of QLEED to find atomic positions below the third atomic layer and on the ability to grow continuous films of six or more layers. Although vacuum deposition of metal films often starts with growth of islands, which give a poor surface for electron diffraction, the islands are coherent with the substrate and as deposition continues the spaces between the islands frequently fill in, hence terraces of six or more layers can then be produced which give acceptable diffraction patterns.

The purpose of this work is to classify different cases of pseudomorphic epitaxy and to describe and apply a simple procedure for evaluation of the complete strain tensor by crystal elasticity theory in the linear approximation. The procedure is applied to examples of more general pseudomorphic epitaxy than the usual similar film and substrate surface unit meshes. See Sec. II for definitions of the cases of pseudomorphic epitaxy. In the general case the film surface unit mesh and substrate surface unit mesh are different in all structural components and the mismatch determines the three in-plane components of strain. We have previously discussed two special cases of pseudomorphic epitaxy[2] and given the quantitative formulation of the general case without applications.[3]

The procedure for calculating the three out-of-plane components is described in Sec. III and applied to two examples of general pseudomorphic epitaxy observed in recent QLEED studies in Sec. IV. A survey of bcc and fcc surfaces of metals with Miller indices up to four found a number of paired bcc and fcc surfaces which match geometry closely enough to be good prospects for general pseudomorphic epitaxy. The strains in one of these pairs are studied quantitatively in Sec. IV and also used to illustrate a generalization to general pseudomorphic epitaxy of the concept of epitaxial lines, which we have previously discussed for pseudomorphic epitaxy of cubic {001} surfaces on cubic {001} substrates.[4] Epitaxial lines are a useful way to show the geometrical effects of pseudomorphic epitaxy for a given pair of surfaces as the scale of the substrate mesh changes while the film remains the same. Remarks on the possible richness of general pseudomorphic epitaxial systems and the value of strain measurements on such systems appear in Sec. V.

II. CASES OF PSEUDOMORPHIC EPITAXY

It is convenient to distinguish different cases of pseudomorphic epitaxy, since the less general cases can be treated more simply. Following the classification given in Ref. 2, we define as case 1 epitaxy the most commonly studied type of epitaxial system. In case 1 epitaxy the film unit mesh and the substrate unit mesh to which the

0163-1829/95/51(8)/5263(6)/$06.00

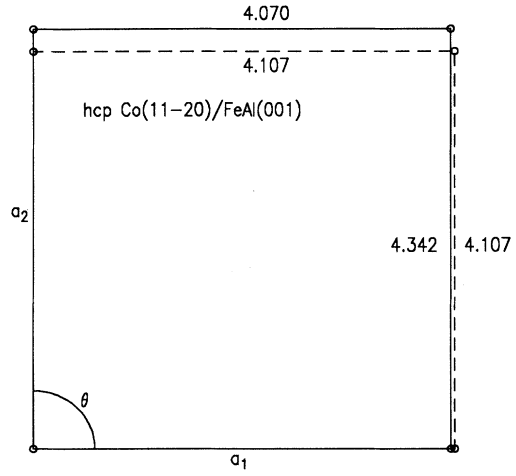

FIG. 1. Scale drawing of the equilibrium rectangular unit mesh of a film of hcp Co($11\bar{2}0$) (solid line) superposed with common origin and collinear smaller sides (a_1) on a square two-atom unit mesh of a film of FeAl{001} as substrate (dashed lines); distances in Å.

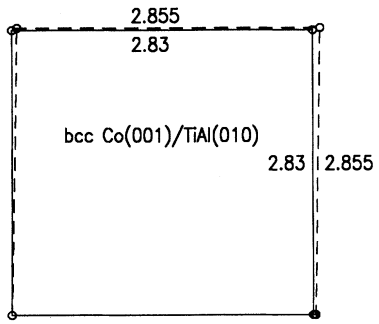

FIG. 2. Scale drawing as in Fig. 1 of square unit mesh of bcc Co{001} film (theoretical values) on rhombic unit mesh of tetragonal TiAl(010) (tetragonal axis along [001]) as substrate ($\theta = 89.068°$).

film unit mesh is strained are similar, i.e., differ only by a scale factor, but have the same angle θ and ratio of sides a_2/a_1. Note that case 1 includes systems where the film and substrate have different crystal structures, but the surface unit meshes are similar, e.g., bcc{001} and fcc{001} or fcc{111} and hcp(0001). Also note that the unit meshes that are matched are not necessarily primitive unit meshes of the film or substrate surfaces. The simplicity of case 1 epitaxy is that a single parameter defines the mismatch and the strain in the plane is isotropic.

There are many examples of case 1 epitaxy where the bulk structure of a sufficiently thick film has been measured by QLEED, thereby permitting a strain analysis. Two instructive examples are (1) fcc Cu{001}/fcc Pd{001} (Ref. 5) (the first metal is the film); the Cu film is shown to have 7% epitaxial tensile strain, hence this system shows that very large strains can be present in the film, at least in the small ordered regions that give LEED spectra; and (2) bcc Fe{001}/fcc Ag{001},[6] which illustrates pseudomorphic epitaxy between similar surfaces belonging to two different crystal structures.

Case 2 pseudomorphic epitaxy is the general case. In case 2 the film unit mesh and substrate unit mesh differ in either or both angle and ratio of sides. The strain in the plane of the film produced by the mismatch has in general three components, and the complete strain tensor in the film will in general have three out-of-plane strain components. Two examples of case 2 epitaxy from our QLEED studies are (1) hcp Co($11\bar{2}0$)/FeAl{001},[7] in which the rectangular primitive unit mesh of hcp Co($11\bar{2}0$) (the primitive unit mesh has a basis of two atoms) is matched to a nonprimitive two-atom unit mesh of FeAl{001} [FeAl has the CsCl structure; the surface actually has eight layers of bct (body-centered-tetragonal) Co(001) on it with the same surface mesh as the FeAl{001}]; Fig. 1 shows the matching unit meshes drawn to scale; the conventional orientation of the unit meshes in Fig. 1, used later in calculating the mismatch strains, labels the shorter sides a_1 and superposes them; and (2) bcc Co{001}/TiAl(010),[8] in which the square primitive unit mesh of bcc Co{001} is matched to the rhombic primitive unit mesh of TiAl(010) (TiAl has the CuAuI structure, which is tetragonal; the (010) bulk layers are half Ti and half Al, but the (010) surface layer is all Al and has a rhombic primitive unit mesh); Fig. 2 shows the unit meshes drawn to scale. The quantitative results of the strain analysis are given in Sec. IV for these systems.

Additional possible case 2 epitaxial systems were found by looking for crystal surfaces with unit mesh parameters that are nearly the same. Examination of bcc and fcc surfaces of metals with Miller indices up to four revealed a number of likely possibilities with sides a_1 and a_2 mismatched by a few percent and differences in angle of only a few degrees. Table I lists some of the possible met-

TABLE I. Selected pairs of metal surfaces with matching unit meshes; first metal is bcc, second is fcc, percent differences in a_1 and a_2 follow the second metal values; distances in Å, θ in degrees.

System	bcc metal a_1	bcc metal a_2	bcc metal θ	fcc metal a_1	fcc metal a_2	fcc metal θ
Fe{310}/Au{311}	2.866	4.753	72.45	2.884(0.6%)	4.996(5.1%)	73.22
Cr{310}/Au{311}	2.885	4.784	72.45	2.884(−0.03%)	4.996(4.4%)	73.22
Zr{310}/Pb{311}	3.607	5.982	72.45	3.500(−3.0%)	6.062(1.3%)	73.22
Ta{411}/Sc{420}	4.675	5.482	64.76	4.533(−3.1%)	5.552(1.3%)	65.90
Cr{411}/Au{420}	4.080	4.784	64.76	4.079(−0.02%)	4.996(4.4%)	65.90
Zr{411}/Th{420}	5.101	5.982	64.76	5.084(−0.33%)	6.226(4.1%)	65.90

al pairs. Either member could be the film and the other the substrate. Quantitative results for the first pair in Table I are given in Sec. IV. Consideration of higher-index surfaces and nonprimitive unit meshes would find many more combinations.

In case 3 epitaxy a set of film rows has a spacing that matches closely the spacing of a set of substrate rows. The film takes an orientation that makes the matching rows of film and substrate parallel to each other and the film is strained in the direction perpendicular to the rows to acquire the substrate row spacing. Zero stress is assumed in the direction parallel to the rows, so that the atomic positions along the rows are not coherent. This case has been treated at length in Ref. 2, where the most favorable orientations are found by minimizing the strain energy.

Both case 1 and case 3 are specializations of case 2. Thus case 1 simply uses a single isotropic strain in the plane of the film and case 3 is approached by matching unit meshes of increasing length parallel to the rows. This paper will discuss only examples of case 2 epitaxy.

III. THE COMPLETE STRAIN TENSOR IN THE FILM

The calculation of the three out-of-plane strain components from the three in-plane components can be formulated as follows. Primes are used to indicate quantities referred to unit surface axes $\hat{\mathbf{x}}'_i$, $i=1-3$ where $\hat{\mathbf{x}}'_1,\hat{\mathbf{x}}'_2$ are in the plane of the film and $\hat{\mathbf{x}}'_3$ is perpendicular to the plane. Let $\varepsilon'_{ij},\sigma'_{ij}$ $(i,j=1-3)$ be the components of strain and stress tensors, respectively, referred to the surface axes. Then $\varepsilon'_{11},\varepsilon'_{12}=\varepsilon'_{21},\varepsilon'_{22}$ give the in-plane strain components and $\varepsilon'_{13}=\varepsilon'_{31}$, $\varepsilon'_{23}=\varepsilon'_{32},\varepsilon'_{33}$ the out-of-plane strain components. The in-plane strain components are determined by the mismatch between film and substrate unit meshes and will be related explicitly below to the unit mesh parameters; the out-of-plane strain components are to be found. The in-plane stress components are unknown, but the three out-of-plane stress components must all vanish because all forces exerted by the substrate on the film are in the plane. Hence three linear stress-strain equations can be solved for the three unknown strain components, i.e.,

$$0=\sum_{k,l=1}^{3} c'_{ijkl}\varepsilon'_{kl}, \quad ij=13,23,33 \tag{1}$$

where the c'_{ijkl} are the components of the rank-four elastic constant tensor referred to the surface axes. Note that since Eqs. (1) are homogeneous in the elastic constants, the dependence of the out-of-plane strain components on film elastic constants enters only through ratios of elastic constants.

The conceptual formulation given above shows that the calculation of out-of-plane strain components from the mismatch is a well-defined solvable problem. However, in the actual computation it is more convenient to transform the second-rank strain and stress tensors to the crystal axes, where the elastic constants are known. The stress-strain equations are applied in the crystal system, and the strain tensors are then transformed back to the surface system. This computation will now be described.

Let a_1^f,a_2^f,θ^f be the equilibrium unit mesh parameters of the film, and a_1^s,a_2^s,θ^s the parameters of the substrate surface. Take $\hat{\mathbf{x}}'_1$ along a_1^s, $\hat{\mathbf{x}}'_2$ perpendicular to $\hat{\mathbf{x}}'_1$, in the plane, and the vector product defines $\hat{\mathbf{x}}'_3=\hat{\mathbf{x}}'_1\times\hat{\mathbf{x}}'_2$ perpendicular to the plane. Then the in-plane strains when the film unit mesh is strained to the substrate unit mesh are

$$\varepsilon'_{11}=(a_1^s/a_1^f)-1\ , \tag{2}$$

$$\varepsilon'_{12}=(a_2^s\cos\theta^s/a_2^f\sin\theta^f-a_1^s\cos\theta^f/a_1^f\sin\theta^f)/2\ , \tag{3}$$

$$\varepsilon'_{22}=a_2^s\sin\theta^s/a_2^f\sin\theta^f-1\ . \tag{4}$$

Equations (2)–(4) are derived in Ref. 3 by linear transformation of the film unit mesh into the substrate unit mesh.

To find a solution of the elastic equations for a strain tensor which has the values of the three in-plane strain components given by Eqs. (2)–(4) and satisfies the vanishing stress conditions of Eq. (1), consider three canonical situations which each have a single in-plane stress component of unit value, i.e., $\sigma'_{11}=1$, or $\sigma'_{22}=1$, or $\sigma'_{12}=\sigma'_{21}=1$; in each case all other components of stress are taken to vanish. We find the complete strain tensor in each canonical case and superpose the three strain tensors with appropriate weights to give the desired in-plane strain components.

The procedure is as follows. Transform the three canonical stress tensors to unit orthogonal crystal axes by the tensor transformation law[9]

$$S_{ij}=\sum_{k,l=1}^{3} x'_{ki}x'_{lj}S'_{kl}\ , \tag{5}$$

where S_{ij} (unprimed) and S'_{ij} are components of a typical second-rank tensor referred to crystal axes and surface axes, respectively, and x'_{ki} is the component of the unit surface axis $\hat{\mathbf{x}}'_k$ along the unit crystal axis $\hat{\mathbf{x}}_i$. The three canonical strain tensors in the crystal axes then satisfy the linear elastic equations

$$\sigma_{ij}=\sum_{k,l=1}^{3} c_{ijkl}\varepsilon_{kl}, \quad i,j=1-3\ . \tag{6}$$

The ε_{kl} found by solving Eqs. (6) for each canonical stress are then transformed back to the surface axes by the inverse transformation formula

$$S'_{ij}=\sum_{k,l=1}^{3} x'_{ik}x'_{jl}S_{kl}\ . \tag{7}$$

Three equations for the three weights of the canonical strain tensors in the surface axes are obtained by putting the weighted sum of the values of $\varepsilon'_{11},\varepsilon'_{12},\varepsilon'_{22}$ in the canonical strain tensors equal to the values of those components produced by the mismatch from Eqs. (2)–(4). The weighted sums of the out-of-plane components of the canonical strain tensor $\varepsilon'_{13},\varepsilon'_{23},\varepsilon'_{33}$ then give the out-of-plane components of the complete strain tensor in the film.

When the complete strain tensor in the film is known in the surface axes, it is also known in the crystal axes.

Then the strain energy density E/V can be evaluated from

$$E/V=\tfrac{1}{2}\sum_{i,j,k,l=1}^{3} c_{ijkl}\varepsilon_{ij}\varepsilon_{kl}\ , \tag{8}$$

where E is the strain energy per atom and V is the volume per atom and the ε_{ij} are now the weighted sums of the canonical strain components in the crystal axes.

A FORTRAN program which solves for the out-of-plane strain components and the strain energy density in case 1 is given in Ref. 2. The program is easily modified to solve case 2 by replacing the values of $\varepsilon'_{11},\varepsilon'_{22},\varepsilon'_{12}$ of case 1 ($\varepsilon'_{11}=\varepsilon'_{22}=a_1^s/a_1^f=a_2^s/a_2^f$, $\varepsilon'_{12}=0$) by the values given by Eqs. (2)–(4). In place of the one-parameter mismatch of case 1, the a_1,a_2,θ values of film and substrate must be entered and Eqs. (2)–(4) used. The program uses the reduced (two-index) form of the elastic constants c and single-index forms of σ and ε in Eq. (6), which are transformed to double-index forms to apply Eqs. (5) and (7).

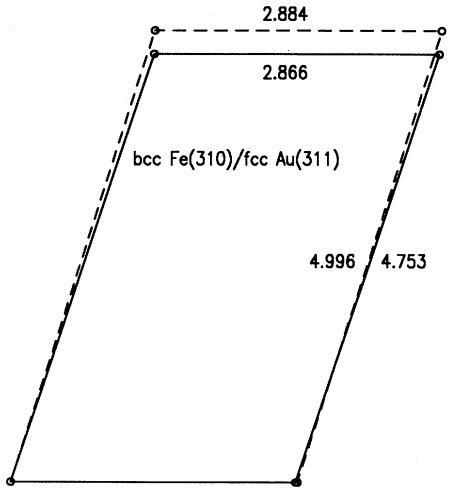

FIG. 3. Scale drawing as in Fig. 1 of unit mesh of bcc Fe{310} film on unit mesh of fcc Au{311} as substrate.

IV. APPLICATIONS OF THE STRAIN TENSOR IN CASE 2 EPITAXY

Results of strain calculations on the two systems mentioned in Sec. II and shown in Figs. 1 and 2, which were found by QLEED to be examples of case 2 epitaxy, will now be given and compared with experiment. Calculated results will also be given for the first system listed in Table I; the corresponding primitive unit meshes of film and substrate are drawn to scale in Fig. 3.

Table II shows the measured and calculated values of the bulk layer spacing d_b under epitaxial strain for the films of hcp Co, bcc Co, and the calculated values of d_b for bcc Fe, and the calculated in-plane and out-of-plane strains. The strained values of d_b differ from the equilibrium-phase layer spacings, but agree with the measured values within experimental error. The hcp Co case has well-known measured lattice constants[10] and elastic constants;[11] however, the bcc Co values are theoretical.[12,13] The lattice constants and elastic constants used in the three strain calculations reported here are listed in Table III. Table III shows that the system bcc Fe{310}/fcc Au{311} (Fig. 3) has values of in-plane strain $\varepsilon'_{11},\varepsilon'_{12},\varepsilon'_{22}$ which are of similar magnitude as the in-plane strains of the hcp Co(11$\bar{2}$0)/FeAl{001} system.

A useful representation of the results of epitaxial strain in this system is to plot a relation which we have called the epitaxial line.[4] In case 1 epitaxy of bcc{001} and fcc{001} films, which produces tetragonal distortions of the cubic structure, the epitaxial line results from the plot of the volume per atom V versus the aspect ratio c/a. In Ref. 4 we have plotted epitaxial lines for bcc Fe{001} and fcc Fe{001} on cubic{001} substrates. A simple generalization of the epitaxial line to case 2 epitaxy is to plot V

TABLE II. Bulk layer spacings d_b for case 2 epitaxial systems; d_s^{eq} is the equilibrium layer spacing of the unstrained crystal; d_b^{meas} is the result of QLEED analysis; d_b^{el} is the elastic theory value of the bulk layer spacing calculated by the procedure of Sec. III; distances in Å.

	hcp Co(11$\bar{2}$0)/FeAl{001}	bcc Co{001}/TiAl(010)	bcc Fe{310}/Au{311}
d_b^{eq}	1.2535	1.415[a]	0.9119
d_b^{meas}	1.29±0.02[b]	1.40[c]	
d_b^{el}	1.27[d]	1.39[e]	0.88
ε'_{11}	0.91%	0.88%	0.62%
ε'_{12}	0.00%	0.81%	0.00%
ε'_{22}	−5.41%	0.87%	5.53%
ε'_{13}	0.00%	0.00%	0.00%
ε'_{23}	0.00%	0.00%	−1.53%
ε'_{33}	1.31%	−0.85%	−3.09%

[a]Theoretical value from first-principles total-energy minimum of $E(V)$; probably 1% lower than experiment; see Ref. 12.
[b]From Ref. 7.
[c]From Ref. 8.
[d]Recalculated; Ref. 7 found $d_b^{el}=1.30$ Å.
[e]Calculated with the theoretical values of B and G from Refs. 12 and 13.

TABLE III. Equilibrium crystal lattice constants and elastic constants (referred to crystal axes) used for strain analysis; distances in Å, elastic constants in Mbar.

Film	a	c	c_{11}	c_{12}	c_{13}	c_{33}	c_{44}
hcp Co[a]	2.507	4.070	3.063	1.651	1.019	3.574	0.753
bcc Co[b]	2.83	2.83	3.60	1.75	1.75	3.60	1.43
bcc Fe[a]	2.866	2.866	2.331	1.3544	1.3544	2.331	1.1783

[a]Lattice constants from Ref. 10; elastic constants from Ref. 11. Note: for hcp Co $c_{55}=c_{44}$, but $c_{66}=(c_{11}-c_{12})/2=0.706$; for bcc Fe $c_{44}=c_{55}=c_{66}$.
[b]Lattice constants and bulk modulus from Ref. 12; shear modulus G estimated from Ref. 13.

against an aspect ratio defined by $d_b/A^{1/2}$, where d_b is the bulk layer spacing and A is the area of the unit mesh, hence $A^{1/2}$ is a measure of the average linear dimension of the unit mesh. As the substrate scale is changed, but the unit mesh remains similar, the film cell dimensions move along the epitaxial line; such a line is plotted in Fig. 4 for the system bcc Fe{310}/fcc X{311} as X varies.

Case 2 systems, unlike case 1 systems, will never show zero strain as the scale of the substrate mesh is varied, since no substrate will match perfectly. However, there will be an optimal substrate with a minimum strain energy. Also in Fig. 4 is a plot of the strain energy density as a function of the aspect ratio of the film produced by varying the scale of the fcc{311} unit mesh of the substrate. The film geometry at the energy minimum (energy density 0.3 kbar) then corresponds to the optimal substrate and provides a fiducial point of the epitaxial line. The optimal substrate at $a_1=2.795$ Å produces in-plane strains $\varepsilon'_{11},\varepsilon'_{12},\varepsilon'_{22}=-2.49\%$, 0.00%, 2.27%, which can be compared with the larger strains on a Au{311} substrate in Table II at $a_1=2.884$ Å. Substrates of Ag{311}, Au{311}, and Al{311} all appear close enough to the equilibrium bcc Fe{310} dimensions to provide examples of case 2 epitaxy.

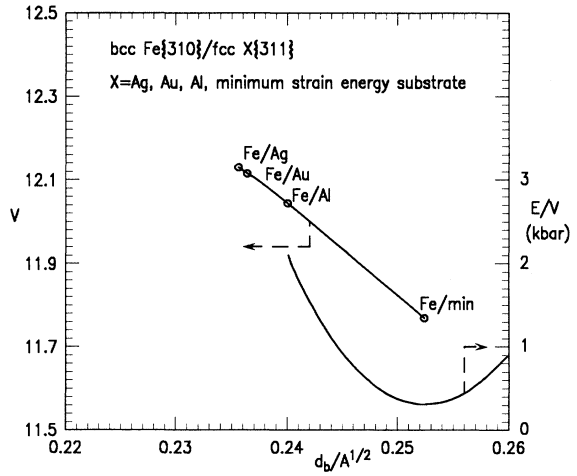

FIG. 4. Epitaxial line (scale on the left) for a film of bcc Fe{310} in pseudomorphic epitaxy on fcc {311} substrates of varying unit mesh size; V is the volume per atom in Å^3; d_b is the bulk layer spacing of the strained film; A is the area of a unit mesh of the strained film. The lower curve is the strain energy density E/V as a function of $d_b/A^{1/2}$ showing a minimum value of 0.6 kbar (scale on the right).

V. DISCUSSION

The main results found here comprise the straightforward solution for the complete bulk strain tensor of the film in the general case of pseudomorphic epitaxy, case 2, and application of the solution. Previous discussions have found partial solutions,[14] such as restriction to case 1 epitaxy or to cubic surfaces. A FORTRAN computer program of 175 lines has implemented the procedure of Sec. III for case 1 epitaxy and appears in Ref. 2; it can be easily adapted to case 2, as described at the end of Sec. III.

Although only a few examples are now known, the number of case 2 epitaxial systems may be large, since there are many crystal structures, many materials with each structure, many surfaces of each crystal, and many unit meshes for each surface if we include nonprimitive unit meshes. The films may also be in metastable phases, which are stabilized by the epitaxial constraint. For metastable phases the information about ratios of elastic constants may not be easily accessible by other techniques.

For crystals of the lowest symmetry, the number of independent elastic constant ratios is 20, but cubic crystals have just two independent ratios, which we can take to be the ratios of the two shear constants $G=(c_{11}-c_{12})/2$ and c_{44} to the bulk modulus B. Consider an epitaxial film with the film plane parallel to any surface of a cubic material in case 1 epitaxy. Then the ratios of the out-of-plane strain components to an in-plane strain component (say ε'_{11}) are independent of the size of the misfit, and are functions of G/B and c_{44}/B only. In Ref. 4 this functional dependence is shown by contours of constant strain ratio of films of fcc{210} in case 1 epitaxy plotted on the G/B, c_{44}/B plane. Since the fcc{210} plane has just one line of reflection symmetry, only one out-of-plane shear strain is nonvanishing, ε'_{23}. Since the lowest-index cubic surfaces {001}, {110}, {111} each have two (or more) lines of reflection symmetry, both ε'_{13} and ε'_{23} vanish for those surfaces. Reference 4 also shows, conversely, that measurement of two strain ratios for a particular cubic film in case 1 epitaxy, e.g., $\varepsilon'_{33}/\varepsilon'_{11}$ and $\varepsilon'_{23}/\varepsilon'_{11}$, determines the elastic constant ratios G/B and c_{44}/B for the material of that film.

In case 2 epitaxy the in-plane strain is not isotropic. The definition of the strain ratios must take account of the anisotropy, e.g., the out-of-plane strains can be divided by the average in-plane strain defined by $\bar{\varepsilon}'\equiv(\varepsilon'_{11}+\varepsilon'_{22})/2$, which is invariant to the choice of sur-

face axes $\hat{x}'_1, \hat{x}'_2$. The strain ratio $\varepsilon'_{33}/\bar{\varepsilon}'$ does not have as clear a meaning in case 2 as in case 1 epitaxy (where it can be considered an epitaxial Poisson ratio), since the ratio in case 2 depends on the size of the mismatch, although the variation with size appears to be moderate when the unit meshes are closely matched.

The strain analysis of pseudomorphic epitaxial film-substrate systems, which depends primarily on QLEED to find the bulk structure of the strained film, is only just beginning. As yet no example of out-of-plane shear strain has been found, and very few bulk strains of epitaxial films with Miller indices greater than 1 have been measured. As yet there are no good examples of bulk strain measurement with the same film crystal epitaxial on more than one distinct surface, i.e., nonsimilar surfaces. Finding the numerous elastic constant ratios for crystals of less than cubic symmetry will require use of more than one substrate surface for films of that crystal. As yet only one elastic constant ratio for a particular crystal has been found, i.e, one Poisson ratio (see, for example, Ref. 5), whereas even cubic crystals have two independent elastic constant ratios.

Finally we note that a valuable contribution to the study of epitaxial strains is now available from first-principles total-energy self-consistent calculations. Such calculations can find the states of a crystal along the epitaxial line by doing a constrained calculation in which the unit mesh of a particular crystal plane is fixed but the layer spacing and registration are varied to minimize the total energy. Then if the size of the unit mesh is varied, but similarity is retained, the strains produced trace out the epitaxial line. This variation corresponds to pseudomorphic epitaxy of that film on different substrates with similar unit meshes. The nonlinear elastic behavior under epitaxial strain will then be included. Such a calculation for tetragonal states of Cu between the bcc and fcc phases has been made recently.[13]

ACKNOWLEDGMENT

This work was sponsored in part by the National Science Foundation with Grant No. DMR 9404421.

[1]The term unit mesh will be used for any two-dimensional cell that generates the two-dimensional lattice of a crystal plane by translation; primitive unit mesh will be used to mean the smallest such cell in area.

[2]F. Jona and P. M. Marcus, Crit. Rev. Surf. Chem. (to be published).

[3]P. M. Marcus and F. Jona, J. Phys. Chem. Solids (to be published).

[4]P. M. Marcus and F. Jona, Surf. Rev. Lett. **1**, 15 (1994).

[5]H. Li, S. C. Wu, D. Tian, J. Quinn, Y. S. Li, F. Jona, and P. M. Marcus, Phys. Rev. B **40**, 5841 (1989).

[6]H. Li, Y. S. Li, J. Quinn, D. Tian, J. Sokolov, F. Jona, and P. M. Marcus, Phys. Rev. B **42**, 9195 (1990).

[7]C. P. Wang, S. C. Wu, F. Jona, and P. M. Marcus, Phys. Rev. B **49**, 17 391 (1994).

[8]S. K. Kim, F. Jona, and P. M. Marcus, Phys. Rev. B **51**, 5412 (1995).

[9]J. F. Nye, *Physical Properties of Crystals* (Clarendon Press, Oxford, 1957), p. 11.

[10]A. Taylor and Brenda Kagle, *Crystallographic Data on Metal and Alloy Structures* (Dover, New York, 1963).

[11]Experimental values are from *Single-Crystal Elastic Constants and Calculated Aggregate Properties: A Handbook,* 2nd ed., edited by C. Simmons and H. Wang (MIT Press, Cambridge, MA, 1971).

[12]Tables of theoretical values for lattice constants and bulk moduli for 3*d* and 4*d* transition elements in both bcc and fcc structures calculated with the augmented spherical wave method can be found in the chapter by V. L. Moruzzi and P. M. Marcus, in *Handbook of Magnetic Materials,* edited by K. H. J. Buschow (Elsevier, New York, 1993), Vol. 7.

[13]T. Kraft, P. M. Marcus, and M. Scheffler in a study of tetragonal states of metals have found bcc Co to be metastable with a finite value of G (unpublished).

[14]F. Witt and R. W. Vook, J. Appl. Phys. **36**, 2169 (1965); **39**, 2773 (1968); J. Hornstra and W. J. Bartels, J. Cryst. Growth **44**, 513 (1978); A. Segmüller and M. Murakami, in *Analytical Techniques for Thin Films,* edited by K. N. Tu and R. Rosenberg (Academic, Boston, 1991).